Understanding the Form of the Input pressure of Focused Ultrasound in the Rayleigh-Plesset Equation to Improve Drug Delivery Efficiency

Peng, Q.; Rottschäfer, V.

DOI
10.1007/978-3-031-55315-8_31

Publication date
2024

Document Version
Final published version

Published in
Computer Methods in Biomechanics and Biomedical Engineering II

Understanding the Form of the Input pressure of Focused Ultrasound in the Rayleigh-Plesset Equation to Improve Drug Delivery Efficiency

Qiyao Peng[1(✉)] and Vivi Rottschäfer[1,2]

[1] Mathematical Institute, Leiden University, Niels Bohrweg 1, Leiden 2333 CA, The Netherlands
q.peng@math.leidenuniv.nl
[2] Korteweg-de Vries Institute for Mathematics, University of Amsterdam, Science Park 105-107, 1098 XG Amsterdam, The Netherlands

Abstract. To improve the drug delivery efficiency in the brain, the combination of the focused ultrasound (FUS) with microbubbles (MBs) shows a great potential to increase the permeability of the blood-brain barrier (BBB). The Rayleigh-Plesset equation is widely used to describe the dynamics of the MB, however, it is not clear what the most promising form of the FUS should be. In this manuscript, we investigate the choice of the input pressure of the FUS, both from analytical and numerical perspective. Furthermore, sensitivity tests are conducted to investigate the relations between the oscillation of the MB and the parameters. We conclude that the average of the FUS should lie at zero, since the MB must expand compared to its initial radius to release the drug molecules.

Keywords: Microbubbles · focused ultrasound · drug delivery · Rayleigh-Plesset equation

1 Introduction

Many existing drugs are aimed at targets present in the brain. However, the blood-brain barrier (BBB) is a major barrier protecting the brain; it limits the transport of drugs from the blood into the brain. The BBB consists of endothelial cells that are connected by tight junctions between the neighboring cells. To increase the permeability of the BBB, and hence, drug delivery into the brain, it is known that inserting microbubbles (MBs) into the blood stream and applying focused ultrasound (FUS) shows great potential [6]. MBs are microspheres filled with gas which is surrounded by a lipid, protein or polymer shell, or so-called coat. Drug molecules can be loaded on this coat, embedded in the coat matrix or even loaded inside the MBs — depending on the material of the coat (see [14] for more details). FUS is a non-invasive therapy that uses high-energy sound waves (at least 1000 times larger than the ultrasound used in the diagnostic imaging). Under the impact of FUS, the MBs start to oscillate. If the input pressure of

W. Skalli et al. (Eds.): CMBBE 2023, LNCVB 39, pp. 280–288, 2024.
https://doi.org/10.1007/978-3-031-55315-8_31

the FUS is in a proper range, then the MBs perform a stable, periodic growth and compression, such that pores are formed on the membrane of the coat to release the drug molecules [13]. Hence, the MBs release the drug molecules in the targeted region. Moreover, this oscillation of the MBs increases the permeability of the BBB via mechanical effects [6].

In particular, when the MBs are really close to the BBB, the oscillation of the MBs give "massages" on the membrane of endothelial cells of the BBB and causes local fluid jets, which is known as microstreaming. As a result, small, temporary openings occur in the endothelial cell membrane, and the tight junctions between the cells are disrupted [6,11]. Hence, drug molecules will cross the BBB easier to enter the targeted region in the brain. However, if the input pressure of the FUS is too large, the MBs will collapse, causing violent mechanical forces that result in cell death and damage to the BBB.

Most modelling work on MBs analyzed the relation between the radius of the MBs and the pressure from the FUS under the assumptions that the MBs are not moving and the FUS is continuously applied. However, MBs migrate to the target region via the arteries and the blood circulation. In other words, the blood flow in the capillaries is the main means by with the MBs move. Depending on the geometry of the MB, the oscillations of the MBs has been studied taking by different approaches. The Rayleigh-Plesset equation is usually utilized in case the MB is a sphere [4,6]. In *in-vitro* experiments, it is more realistic to look at MBs that are not spherically symmetric, where usually the impact of the capillary on the shape of MBs is also taken into account. Then the Navier-Stokes equation, combined with the immersed boundary approach [12], is implemented in a numerical model [7–9]. So far, most work has focused on reproducing the geometry of the MBs that are recorded in the laboratory, rather than considering how to apply this approach in the clinical practice. Of course, this is still faced with many challenges but is essential for future application of the method. One of the aspects that needs further study is concerned with the parameters in the model, and more specifically, the form of the input FUS pressure.

In this manuscript, we will discuss the form of the input FUS pressure, and carry out some sensitivity tests to investigate how the parameters affect the oscillation and the average radius of the MBs. This will be beneficial to have a better insight into the model and to determine the range of the parameter values. The manuscript is structured as below: Sect. 2 introduces the Rayleigh-Plesset equation and some mathematical analysis on the equation is presented in Sect. 3. Then, we show the numerical results, particularly the sensitivity tests in Sect. 4. Finally, Sect. 5 delivers the conclusions.

2 Rayleigh-Plesset Equation

The most commonly used nonlinear equation of motion describing the oscillation of a MB in an infinite volume of liquid is the Rayleigh-Plesset (RP) equation [2]. Neglecting the thermal effect caused by the oscillation of the MBs, the authors in [4] simplified the complete RP equation

$$\rho\left(R\ddot{R}+\frac{3}{2}\dot{R}^2\right)=\left(p_0+\frac{2\sigma(R_0)}{R_0}\right)\left(\frac{R}{R_0}\right)^{-3\kappa}\left(1-\frac{3\kappa}{c}\dot{R}\right)-\frac{2\sigma(R)}{R}-\frac{4\mu\dot{R}}{R}-p_0-p_A(t), \quad (1)$$

which describes the change of the radius of the MB. Here, $R, \dot{R}, \ddot{R}$ represent the radius, velocity and acceleration of the microbubble wall, R_0 is the initial radius of the microbubble, ρ is the fluid density, p_0 is the ambient pressure, $\sigma(R)$ is the surface tension, κ is the polytropic gas exponent, μ is the fluid dynamical viscosity, c is the speed of the sound, and $p_A(t)$ is the applied pressure of FUS. The surface tension σ depends on the radius of the MB and the material of the coat, so far, we take the surface tension to be zero. Hence, this reduces Eq. (1) to

$$\rho\left(R\ddot{R}+\frac{3}{2}\dot{R}^2\right)=p_0\left(\frac{R}{R_0}\right)^{-3\kappa}\left(1-\frac{3\kappa}{c}\dot{R}\right)-\frac{4\mu\dot{R}}{R}-p_0-p_A(t), \quad R(0)=R_0, \quad \dot{R}(0)=0. \quad (2)$$

In most modelling work on MBs, it has been assumed that the input pressure from FUS takes the form of a periodic function, with angular frequency $2\pi f$, where f is the frequency of FUS pressure. However, whether the mean of the input pressure is zero or not is not clear. In this manuscript, we consider the input pressure to be

$$p_A(t)=C_0+C_1\sin(2\pi f t)$$

for constants C_0 and C_1 where $C_0, C_1 \geqslant 0$. Here, C_0 is the average input pressure and C_1 the amplitude of the oscillation around C_0 (both in kPa).

Due to the large difference between the parameter values in the equation, we first non-dimensionalize the equation by defining the following rescalings:

$$R^*=\frac{R}{2R_0},\ t^*=tf,\ c^*=\frac{c}{2R_0 f}, \rho^*=\frac{\rho}{\rho_l},\ p^*=\frac{p}{(2R_0)^2 f^2 \rho_l},\ \mu^*=\frac{\mu}{(2R_0)^2 f \rho_l},$$

where ρ_l is the density of the fluid. The system becomes dimensionless and we obtain

$$\rho^*\left(R^*\frac{\partial^2 R^*}{\partial(t^*)^2}+\frac{3}{2}\left(\frac{\partial R^*}{\partial t^*}\right)^2\right)=p_0^*\left(2R^*\right)^{-3\kappa}\left(1-\frac{3\kappa}{c^*}\left(\frac{\partial R^*}{\partial t^*}\right)\right)-\frac{4\mu^*}{R^*}\left(\frac{\partial R^*}{\partial t^*}\right)-p_0^*-p_A^*(t^*), \quad (3)$$

where $R^*(0)=\frac{1}{2}$ and $\left.\frac{dR^*}{dt^*}\right|_{t^*=0}=0$. After non-dimensionalization,

$$p_A^*(t^*)=C_0^*+C_1^*\sin(2\pi t^*),$$

In case no FUS is applied on the MB, that is, $p_A^*(t)=0$, the equilibrium radius is the same as the initial radius of MBs. However, applying FUS with $C_0^* \neq 0$ on the MBs results in a new equilibrium, around which the MB will start to oscillate. In the following, we will conduct the mathematical analysis in the dimensionless model. To avoid confusion and have a better insight into the parameters, the numerical results will be presented in the dimensional variables.

3 Mathematical Analysis

In this section, we determine the steady state solution to Eq. (3) to obtain a better insight into the equation. We start with a constant input pressure from the FUS only. Thus, we assume $C_1^* \equiv 0$ so that $p_A^*(t) \equiv C_0^*$. Then we assume the solution to be $R^*(t) = \tilde{R}^*$, where $\tilde{R}^*$ is constant and substitute this into Eq. (3). This yields

$$0 = p_0^*(2\tilde{R}^*)^{-3\kappa} - p_0^* - C_0^*,$$

and the steady state of the radius of the MB is given by

$$\tilde{R}^* = \frac{1}{2}\left(\frac{p_0^*}{p_0^* + C_0^*}\right)^{\frac{1}{3\kappa}}. \tag{4}$$

We conclude that when $C_0^* = 0$ the steady state is at $\tilde{R}^* = \frac{1}{2}$ and $\tilde{R}^* < \frac{1}{2}$ for $C_0^* > 0$, which is smaller than the initial radius of the MB. Stability analysis (not given here) shows that the solution will converge to this steady state for $C_1^* = 0$. Moreover, it can also be shown that solutions will start to oscillate around this steady state when C_1^* is small; this analysis will be presented in a future publication. However, for a larger C_1^*, numerical simulations, as given in the next section, are needed to investigate the behaviour of the solution.

4 Numerical Results

In *in-vitro* experiments, the FUS that is set to certain frequency, is on for a few microseconds and off for another a few microseconds. This on and off procedure of FUS is repeated for few seconds [14]. In this manuscript, we limit ourselves to the case where the FUS is continuously applied on the MBs in the time interval of a few microseconds. Here, we selected this time interval to be $10\,\mu$ s [14]. The parameter values (both dimensional and dimensionless) are shown in Table 1, including the references where we obtained these from. We aim to be able to compare the results to the *in-vivo* and *in-vitro* experiments, therefore, all the numerical results are given in terms of the dimensional variables.

For the choice $C_0 = 110$ kPa and $C_1 = 110$ kPa, the oscillation of the MB radius against time is presented in Fig. 1, where the initial radius of MB is $R_0 = 0.5\,\mu$m. While for both choices of C_0, the same value of C_1 is used, $C_0 = 110$ kPa (in blue) results in an oscillation in which the MB is never larger than its initial size, whereas $C_0 = 0$ kPa leads to an oscillation in which the MB expands and shrinks comparing to its initial size. In other words, $C_0 = 0$ kPa ensures the release of the drug molecules that are loaded on the coat or inside the MB.

To obtain a better insight into the relation between the oscillation and other parameters, sensitivity tests are conducted. In this manuscript, we measure the

Table 1. Parameter values used in this section

Parameter	Description	Unit	Original Value	Dimensionless Value	Ref.
ρ	Blood density	kg/m^3	1025	1	[5]
p_0	Ambient pressure	kPa	110	26.83	[4]
κ	Polytrophic gas exponent	–	1.1	1.1	[4]
c	Sound speed in blood	m/s	1578	785	[1]
μ	Blood (dynamical) viscosity	$kg/(m \cdot s)$	3.5×10^{-3}	1.71	[10]
f	Frequency of FUS pressure	$1/s$	2×10^6	1	[3]
R_0	Initial MB radius	m	0.5×10^{-6}	0.5	[4]
T	Time interval of applying FUS	s	10×10^{-6}	20	[14]

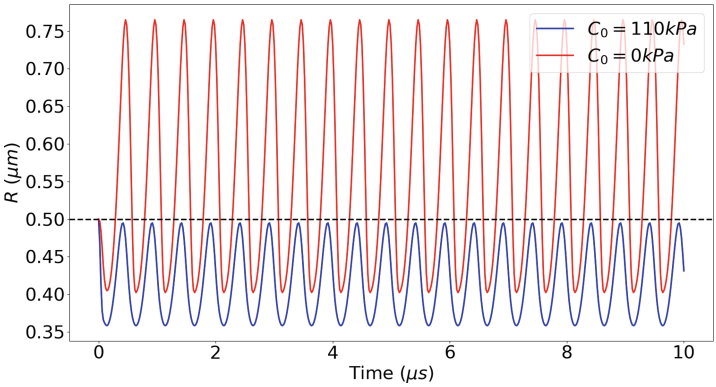

Fig. 1. The solution of Eq. (2) given for $C_0 = 0$ kPa (in red) and $C_0 = 110$ kPa (in blue) where in both cases $C_1 = 110$ kPa, $R(0) = \frac{1}{2}$ and $\dot{R}(0) = 0$. Here, the rest of the parameter values are as given in Table 1.

oscillation of the solution by the relative ratio of the MB with respect to the initial radius, that is,

$$r(t) = \frac{R(t) - R_0}{R_0}. \tag{5}$$

Note that this quotient is the same in the dimensional and dimensionless setting because of the linear rescaling of the radius. This quotient can be either positive or negative, indicating the growth and the shrinkage of the MB, respectively. Moreover, the value indicates how large or small the amplitude of the oscillation is. In Fig. 2, we show the maximum, minimum and average values of $r(t)$ versus the initial radius R_0 for the choices of $C_0 = 110$ kPa (left) and $C_0 = 0$ kPa (right) where $C_1 = 110$ kPa. We also give the steady state that we determined in Sect. 3 in black. We notice that $C_0 = 0$ kPa is more sensitive to the variation of the initial size comparing to $C_0 = 110$ kPa. As the initial radius increases, we observe that the oscillation decreases in both subfigures. Moreover, the average radius of the MB comes closer to the steady state that is found analytically in Sect. 3, and there is even a quite good correspondence between these for the

choice $C_0 = 110$ kPa. Furthermore, we observe that for $C_0 = 110$ kPa, the maximal value of $r(t)$ lies below or slightly above 0, hence, the radius of the MB does not expand compared to the initial state.

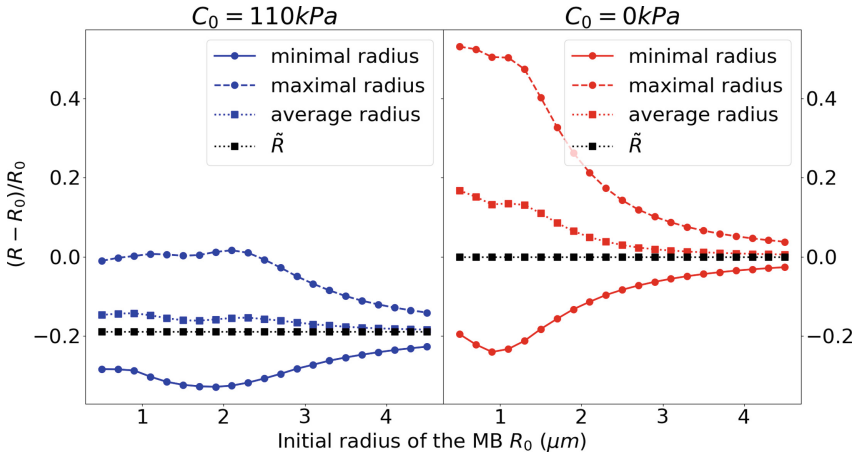

Fig. 2. The maximum (solid), minimum (dashed) and average (dotted) value of the relative change $r(t)$ versus the initial radius R_0 is shown for Eq. (2). Black curves in both subfigures are the relative ratio $r(t)$ of the steady state given by Expression (4). On the left-hand side (blue), the curves are given for $C_0 = 110$ kPa and on the right-hand side (red) $C_0 = 0$ kPa, in both cases, $C_1 = 110$ kPa.

Generally speaking, a larger amplitude of the FUS input pressure causes a larger oscillation and a larger average radius of MB, see Fig. 3. There we again give the maximum, minimum and average radius for $C_0 = 110$ kPa (left) and $C_0 = 0$ kPa (right) but now we vary the amplitude C_1 of the FUS. Similar to the conclusion from Fig. 2, $C_0 = 0$ kPa is more sensitive to the change of the FUS input pressure amplitude than $C_0 = 110$ kPa. This figure also verifies the statement in Sect. 3 that when C_1 is small and $C_0 \geqslant 0$, the MB oscillates around the steady state given in Expression (4), since the average radius and the steady state (in black) are close to each other as long as C_1 is small. Furthermore, when $R_0 = 0.5\,\mu$ m, the amplitude $C_1 = 20$ kPa hardly induces oscillation of the MB (Fig. 3), and in Fig. 2, when $R_0 = 4\,\mu$ m, the amplitude $C_1 = 110$ kPa is not large enough for a comparable oscillation as in the case of $R_0 = 0.5\,\mu$ m. Thus, we infer that for every radius of MB, there exists a range of the FUS input pressure such that MB oscillates.

In Fig. 4, the ambient pressure p_0 is varied for both $C_0 = 110$ kPa (left) and $C_0 = 0$ kPa (right), when $C_1 = 110$ kPa and $R_0 = 0.5\,\mu$ m. As is expected from Expression (4), the steady state $\tilde{R}$ increases parabolically for $C_0 > 0$, when p_0 increases, see the black curve in the left subfigure. According to the numerical analysis, we observe that, opposite to the tendency when $C_0 > 0$, increasing the ambient pressure when $C_0 = 0$ kPa reduces the average radius and amplitude of

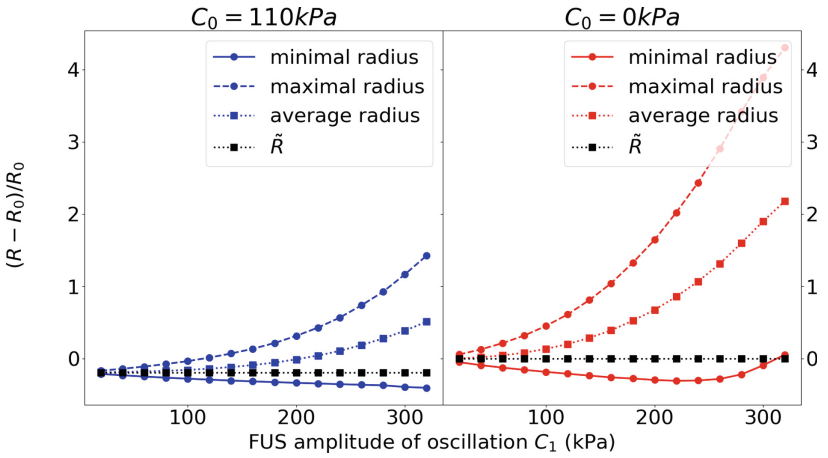

Fig. 3. The maximal (dashed), minimal (solid) and average (dotted) value of $r(t)$ for Eq. (2) versus the amplitude of the FUS for $C_0 = 110$ kPa (left) and $C_0 = 0$ kPa (right), and $R_0 = 0.5\,\mu$m. Black curves in both subfigures represent the steady state given in Expression (4).

the oscillation of the MB. Moreover, it seems that for all p_0 and $C_0 = 110$ kPa, the maximum and minimum of the solution are (more or less) equally far from the average.

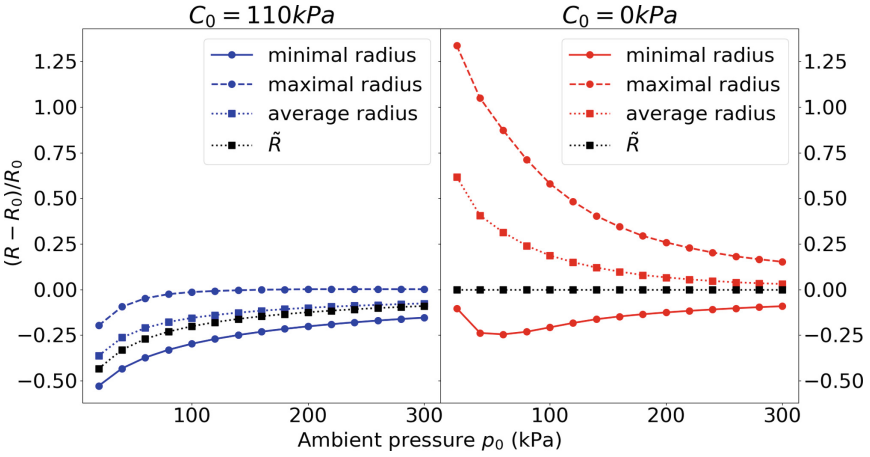

Fig. 4. The minimal (solid line), maximal (dashed) and average (dotted) value of $r(t)$ for Eq. (2) versus the ambient pressure p_0 for $C_0 = 110$ kPa (left) and $C_0 = 0$ kPa (right) where $C_1 = 110$ kPa and $R_0 = 0.5\,\mu$m. Black curves in both subfigures are the value of r for the steady state given in Expression (4).

5 Conclusions

In this manuscript, we investigate the influence of the value of the FUS input pressure C_0 with a focus on whether to take $C_0 = 0$ or $C_0 > 0$. According to the mathematical analysis, when $C_0 > 0$, the average radius of the MB is smaller than the initial radius. Hence, this results in oscillation where the maximum amplitude is not or only barely larger than the initial radius, even though the oscillation still occurs, as is shown in Fig. 1. Turning back to the experimental setting described in the introduction we conclude that as a consequence, the drug molecules cannot be released from the MB [13,14]. Therefore, we conclude that the choice where $C_0 = 0$ kPa is the preferred choice.

Furthermore, various sensitivity tests are conducted regarding to the initial radius of the MB, the FUS input pressure amplitude and the ambient pressure. In general, $C_0 = 0$ kPa is more sensitive to the change of these parameters than $C_0 = 110$ kPa. For any size of MB, there exists a threshold of the amplitude of oscillation C_1 of FUS: if this amplitude is below this threshold, MBs may not be able to release the drug molecules due to the small oscillation. A larger FUS input pressure amplitude leads to a larger average size of the MB and a larger oscillation, which also increases the risk of collapse of the MB. The average value of r for $C_0 > 0$ and $C_0 = 0$ decreases, given an increasing ambient pressure, meanwhile the average radius slowly reaches a steady state as the ambient pressure increases. In summary, this study provides a better insight into the relation between the input pressure of the FUS and the MB radius.

References

1. Aaslid, R.: Cerebral autoregulation and vasomotor reactivity. In: Handbook on Neurovascular Ultrasound, pp. 216–228. KARGER (2006). https://doi.org/10.1159/000092434
2. Bennen, C.E.: Fundamentals of multiphase flow. Cambridge University Press (2005). https://doi.org/10.1017/cbo9780511807169.005
3. Canney, M.S., et al.: Acoustic characterization of high intensity focused ultrasound fields: a combined measurement and modeling approach. J. Acoustical Soc. Am. **124**(4), 2406–2420 (2008). https://doi.org/10.1121/1.2967836
4. de Jong, N., et al.: Ultrasonic characterization of ultrasound contrast agents. Med. Biological Eng. Comput. **47**(8), 861–873 (2009). https://doi.org/10.1007/s11517-009-0497-1
5. Hinghofer-Szalkay, H., Greenleaf, J.E.: Continuous monitoring of blood volume changes in humans. J. Appl. Physiol. **63**(3), 1003–1007 (1987). https://doi.org/10.1152/jappl.1987.63.3.1003
6. Kooiman, K., et al.: Acoustic behavior of microbubbles and implications for drug delivery. Adv. Drug Deliv. Rev. **72**, 28–48 (2014). https://doi.org/10.1016/j.addr.2014.03.003
7. Ma, X., et al.: Numerical simulation of single bubble dynamics under acoustic travelling waves. Ultrason. Sonochem. **42**, 619–630 (2018). https://doi.org/10.1016/j.ultsonch.2017.12.021

8. Madadi-Kandjani, E., Xiong, Q.: Validity of the spring-backed membrane model for bubble-wall interactions with compliant walls. Comput. Fluids **96**, 116–121 (2014). https://doi.org/10.1016/j.compfluid.2014.03.010
9. Mifsud, J., et al.: Numerical simulation of a confined cavitating gas bubble driven by ultrasound. Phys. Fluids **33**(12), 122114 (2021). https://doi.org/10.1063/5.0075280
10. Nader, E., et al.: Blood rheology: Key parameters, impact on blood flow, role in sickle cell disease and effects of exercise. Front. Physiol. **10** (2019). https://doi.org/10.3389/fphys.2019.01329
11. Roovers, S., et al.: The role of ultrasound-driven microbubble dynamics in drug delivery: From microbubble fundamentals to clinical translation. Lang. Muir **35**(31), 10173–10191 (2019). https://doi.org/10.1021/acs.langmuir.8b03779
12. Roy, S., et al.: Immersed boundary method: development and applications. Springer (2020)
13. Sonaye, H.V., et al.: Using microbubbles as targeted drug delivery to improve AIDS. In Pharmaceutical Formulation Design - Recent Practices. IntechOpen (2020). https://doi.org/10.5772/intechopen.87157
14. Wang, T.Y., et al.: Ultrasound and microbubble guided drug delivery: mechanistic understanding and clinical implications. Current Pharmaceutical Biotechnol. **14**(8), 743–752 (2014). https://doi.org/10.2174/1389201014666131226114611